

Supporting Information

Comparison of Perovskite and Perovskite Derivatives for use in Anion-based Pseudocapacitor Applications

Robin P. Forslund¹, Joshua Pender¹, Caleb T. Alexander², Keith P. Johnston² & Keith J. Stevenson^{3*}

¹ Department of Chemistry, The University of Texas at Austin, 1 University Station, Austin, Texas 78712, USA.

² McKetta Department of Chemical Engineering, The University of Texas at Austin, 200 E Dean Keeton St., Austin, Texas 78712, USA.

³ Center for Energy Science and Technology, Skolkovo Institute of Science and Technology, Bolshoi Boulevard 30, Moscow 121205, Russia.

* Corresponding author: K.Stevenson@skoltech.ru

Contents

Figure S1: BET surface area sorption curves	S3
Figure S2: Additional SEM images of $\text{CaMnO}_{3-\delta}$ (CMO) perovskite oxide	S3
Figure S3: Additional SEM images of $\text{Ca}_2\text{MnO}_{4-\delta}$ (CMO RP) Ruddlesden-Popper oxide	S4
Figure S4: Mn 3p XPS analysis	S4
Figure S5: Electrochemical characterization of unreduced $\text{CaMnO}_{3-\delta}$ and $\text{Ca}_2\text{MnO}_{4-\delta}$ materials	S5
Figure S6: PXRD pattern of $\text{SrFeO}_{2.5}$ (SFO)	S5
Figure S7: Two-electrode capacitances measured via CV	S6
Table S1: Electrochemically measured oxygen diffusion rates.....	S6

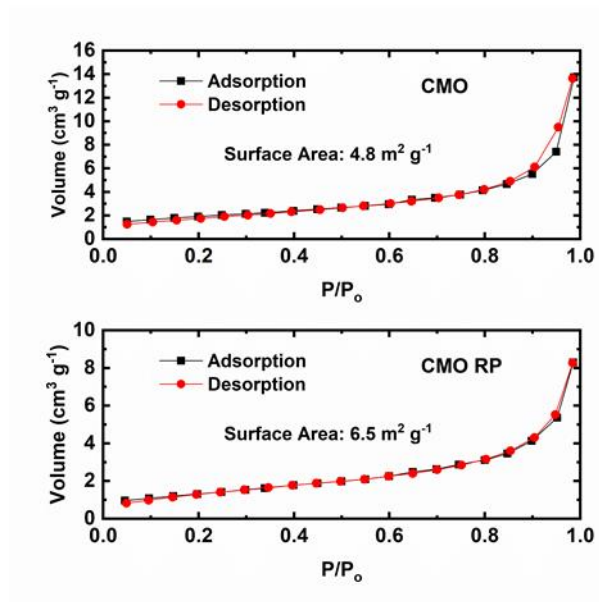


Figure S1. Nitrogen sorption isotherms for BET surface area analysis of unreduced CaMnO_{3.6} (CMO) perovskite and Ca₂MnO_{4.6} (CMO RP) Ruddlesden-Popper oxides.

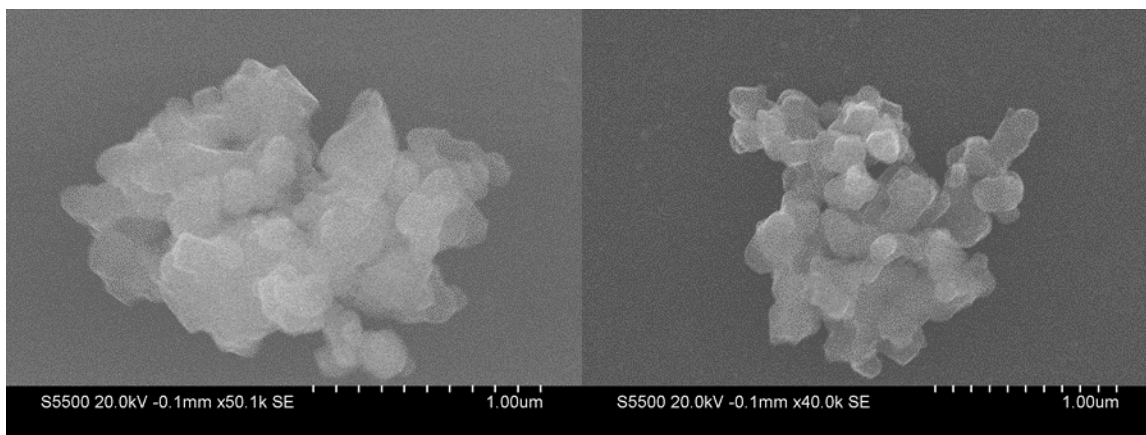


Figure S2. Additional SEM images of CaMnO_{3.6} (CMO) perovskite oxide.

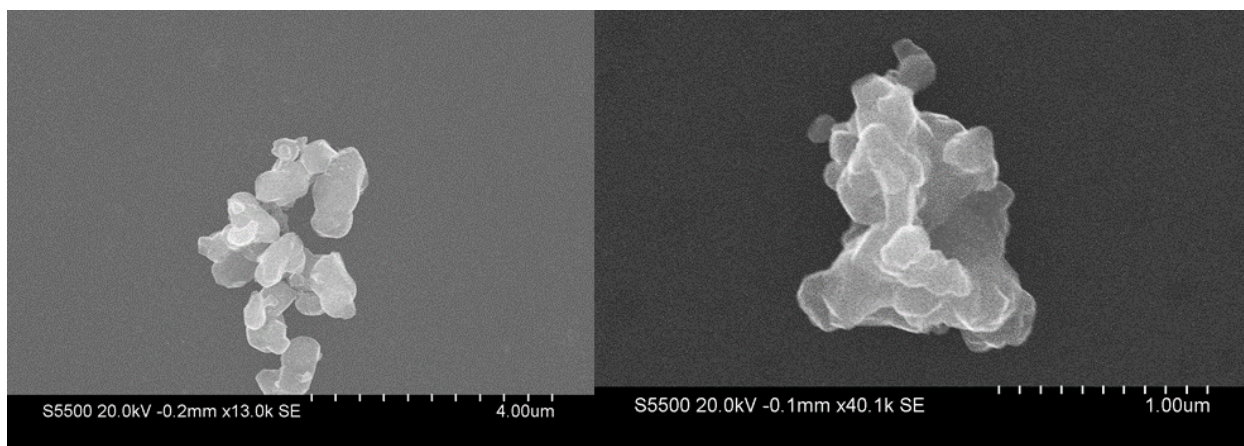


Figure S3. Additional SEM images of $\text{Ca}_2\text{MnO}_{4-\delta}$ (CMO RP) Ruddlesden-Popper oxide.

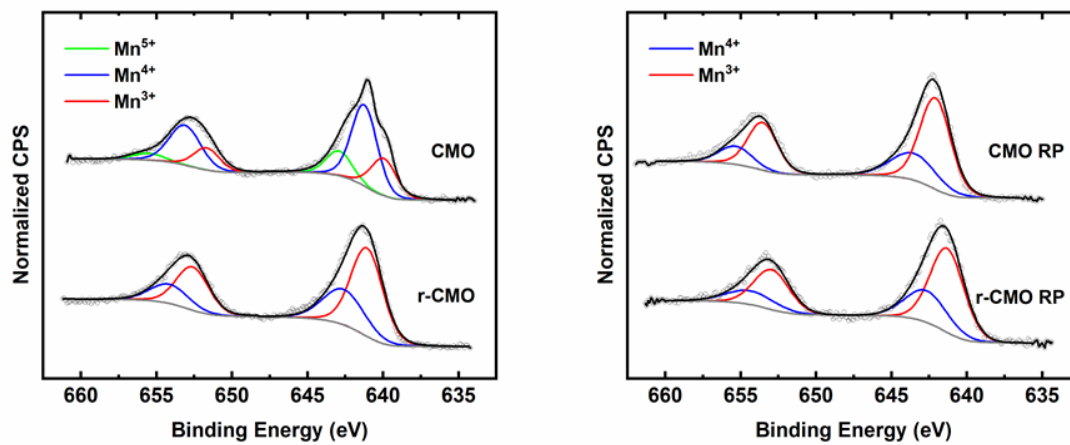


Figure S4. Mn 3p XPS analysis of $\text{CaMnO}_{3-\delta}$ (CMO) perovskite and $\text{Ca}_2\text{MnO}_{4-\delta}$ (CMO RP) Ruddlesden-Popper oxides before and after reduction in a reducing atmosphere of 7% H_2 in Ar at 325° C.

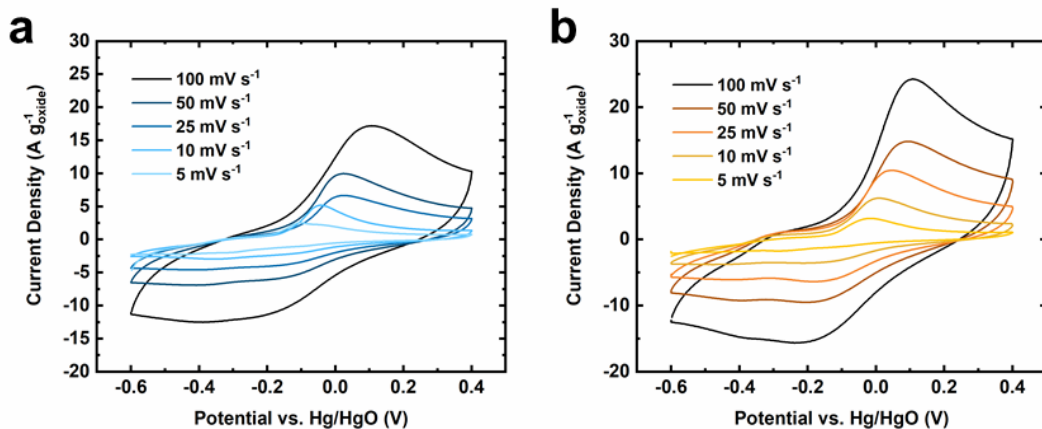


Figure S5. Electrochemical characterization of unreduced $\text{CaMnO}_{3-\delta}$ and $\text{Ca}_2\text{MnO}_{4-\delta}$ materials as pseudocapacitors in a 3-electrode cell. (a) CVs of CMO performed at multiple scan rates over a 1 V window. (b) CVs of CMO RP performed at multiple scan rates over a 1 V window.

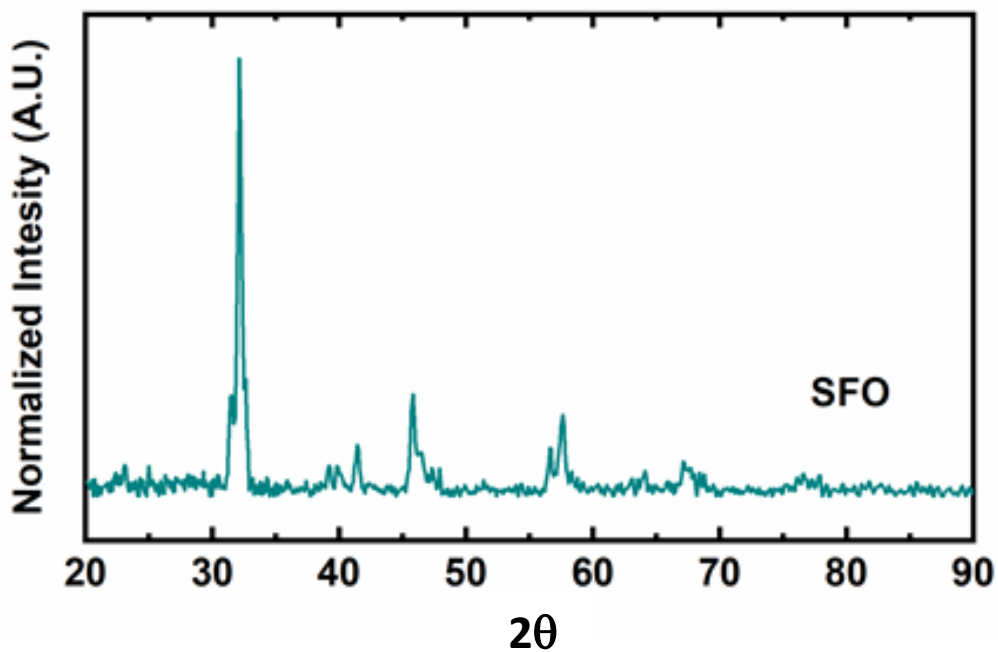


Figure S6. PXRD pattern of $\text{SrFeO}_{2.5}$ (SFO). Reduction of SrFeO_3 perovskite was performed in an atmosphere of 7% H_2/Ar at 325°C to achieve the Brownmillerite phase.

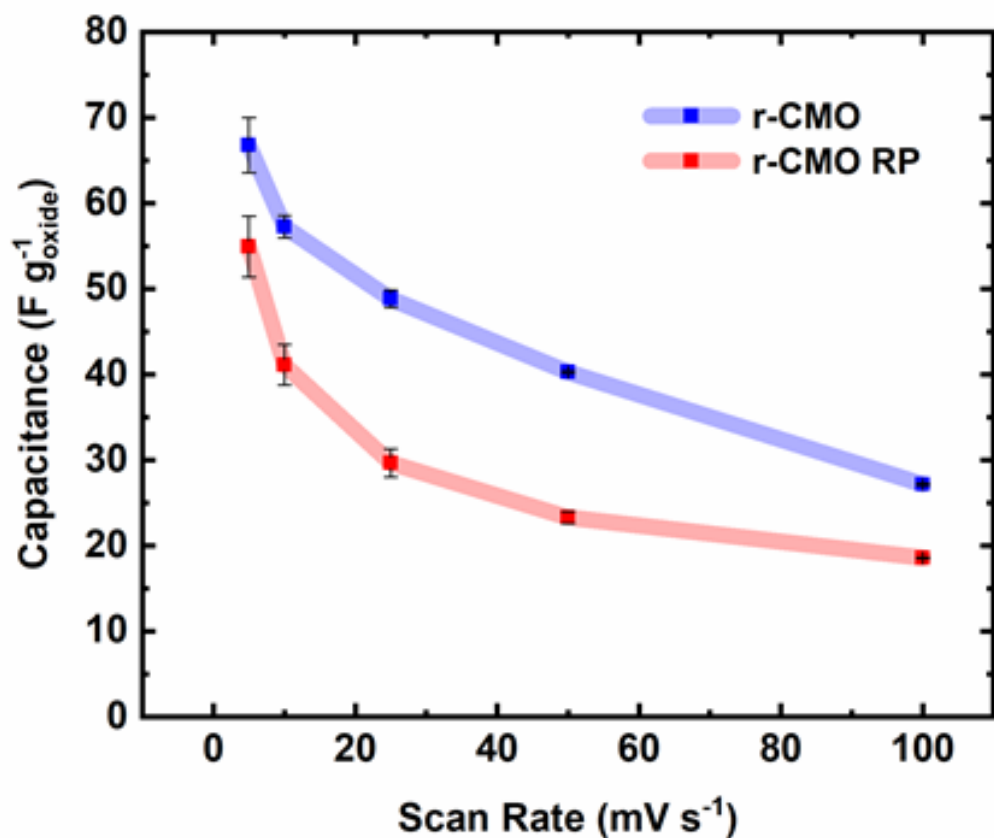


Figure S7. Gravimetric capacitances determined from CVs at various scan rates using SrFeO_{2.5} as the anode material and either r-CMO or r-CMO RP as the cathode material in two-electrode cell asymmetric pseudocapacitor experiments.

Table S1. Electrochemically measured oxygen diffusion rates in CaMnO_{3-δ} (CMO) perovskite and Ca₂MnO_{4-δ} (CMO RP) Ruddlesden-Popper oxides.

Sample	Composition	Intercalation Oxygen Diffusion Rate (cm ² s ⁻¹)	Deintercalation Oxygen Diffusion Rate (cm ² s ⁻¹)
CMO	CaMnO _{3.11}	1.88E-11 ± 5.7E-12	2.44E-11 ± 3.6E-12
r-CMO	CaMnO _{2.53}	2.64E-11 ± 2.8E-12	3.71E-11 ± 1.2E-12
CMO RP	Ca ₂ MnO _{3.92}	3.54E-12 ± 1.4E-12	1.68E-12 ± 3.6E-13
r-CMO RP	Ca ₂ MnO _{3.61}	1.60E-11 ± 8.6E-14	1.44E-11 ± 4.9E-14